Available online at www.sciencedirect.com
SciVerse ScienceDirect
Ceramics International 39 (2013) 2943–2948
CERAMICS INTERNATIONAL
www.elsevier.com/locate/ceramint

Size-controlled synthesis and photoluminescence of porous monolithic α-alumina

Shi-Fa Wang, Xia Xiang*, Qing-Ping Ding, Xiao-Lin Gao, Chun-Min Liu, Zhi-Jie Li, Xiao-Tao Zu*

Department of Applied Physics, University of Electronic Science and Technology of China, Sichuan, Chengdu 610054, China

Received 23 July 2012; received in revised form 20 September 2012; accepted 21 September 2012
Available online 28 September 2012

Abstract

A modified polyacrylamide gel route is used to synthesize porous monolithic α-alumina. X-ray powder diffraction analysis indicates that the as-prepared samples are rhombohedral α-alumina phase, suggesting that high-purity α-alumina can be prepared by using different chelating agents and sintering at about 1150 °C. The scanning electron microscopic images show that the macropore size of the α-alumina samples is related to the chelating agent. The photoluminescence spectra show that a major emission band around 365 nm and a weaker side band located at 330 nm are observed when the excitation wavelength is 228 nm. Interestingly, the intensity of emission peak at 365 nm decreases with the decreasing pore size. The pore-forming and luminescence mechanisms of porous alumina have been discussed based on the experimental results.

Keywords: α-Alumina; Monolithic structure; Chelating agent; Luminescence intensity

1. Introduction

Alumina is an important functional ceramic material with several different metastable phases (boehmite→γ→δ→θ-Al_2O_3) which are eventually converted to stable rhombohedral α-Al_2O_3 phase after calcination at high temperature [1,2]. α-Al_2O_3 is often used as optical fiber and infrared window for extensive applications [3]. It has recently attracted a great deal of interest due to its applications in highly efficient phosphors and dosimeters [3,4]. In addition, the porous anodic alumina is often used as template to prepare photoelectric material and devices such as nanoparticles and nanowires, etc [5,6]. It is well known that the properties of materials strongly depend on their morphologies, dimensions, sizes and defects. Especially, nanostructured Al_2O_3 usually includes nonequilibrium phases, so oxygen nonstoichiometry is possible [3].Therefore, nanoporous α-Al_2O_3 are expected to exhibit enhanced properties or completely new properties which are usually absent in their bulk. From this point of view, it is interesting to prepare and study luminescence properties of the macroporous α-Al_2O_3 powder.

The color centers (F and P centers) often exist in the inner part of the porous Al_2O_3 powder. However, the surface defect levels usually exist on the surface of powder. Generally, the intensity of the emission peaks of nanometer oxide powder decreases with the increasing particle size [7,8]. The number of dangling and unsaturated bonds on the particle surface is heavily dependent on the particle size. The larger particle having a smaller specific surface area, has less dangling and unsaturated bonds on the surface, which will affect the defect levels and luminescence properties of powder [8].

Various methods have been applied to prepare porous Al_2O_3, such as sol-gel method, [9–13] precipitation method, [14] extrusion method, [15–18] centrifugal molding, [19] and replication method [20]. Among them, sol–gel method is very interesting because it is easy to control the topography by using template or organic additives [21–24]. However, the template preparation requires several steps: (1) prepare

*Corresponding authors. Tel./Fax: +86 28 83202130.
E-mail addresses: xiaxiang@uestc.edu.cn (X. Xiang), xtzu@uestc.edu.cn (X.-T. Zu).

0272-8842/$ - see front matter © 2012 Elsevier Ltd and Techna Group S.r.l. All rights reserved.
http://dx.doi.org/10.1016/j.ceramint.2012.09.068

macroporous template with a certain shape, (2) prepare precursor sol, (3) fill the template with precursor sol, (4) remove the template by calcination or etching [25,26]. To date, there has been little work on synthesis of α-Al_2O_3 by using organic additives.

In this work, we present a new route to synthesize monolithic α-Al_2O_3 with citric acid, ethylenediamine-tetraacetic acid (EDTA), tartaric acid or oxalic acid as the chelating agent. To obtain monolithic α-alumina, *N*,*N'*-methylene-bisacrylamide is used as the cross-linking agent. This fabrication method is easy to obtain porous α-Al_2O_3 with adjustable pore size by using different chelating agents. The luminescence properties of the prepared monolithic α-Al_2O_3 have been investigated.

2. Experimental

2.1. Synthesis

Aluminum nitrate, $Al(NO_3)_3 \cdot 9H_2O$ was dissolved in the deionized water to obtain solution of 0.015 mol/l. After the solution was transparent, a stoichiometric amount of chelating agent (citric acid, EDTA, tartaric acid or oxalic acid) was added to the solution in the molar ratio 1.5:1 with respect to the cations (Al) to complex the cations. After that, 20 g glucose was dissolved in the solution. Finally, the acrylamide and N,N′-methylene–bisacrylamide monomers were added to the solution and the pH value was adjusted to ~7 with aqueous ammonia. The resultant solution was heated to 90 °C on a hot plate to initiate the polymerization reaction, and a few minutes later a polyacrylamide gel was formed. The gel was dried at 120 °C for 24 h in a thermostat drier. The obtained xerogel precursor was ground into powder and some powder was sintered at 700, 1000, 1100 and 1150 °C for 2 h to prepare macroporous Al_2O_3 samples.

2.2. Characterization

The phase purity of the samples was measured by means of X-ray powder diffraction (XRD) with Cu Kα radiation. The particle morphology was investigated by an INSPECT-F field-emission scanning electron microscope (SEM). The luminescence properties were investigated at room temperature with a SHIMADZU RF-5301PC fluorescence spectrophotometer in the range of 200–800 nm by using a 150 W xenon lamp as excitation source.

3. Results and discussion

In the polyacrylamide gel route, citric acid is utilized as a chelating agent to complex with the cations to stabilize the solution against hydrolysis or condensation. This chelating agent is suitable for most cations. Generally the appropriate choice of a chelating agent can significantly improve the quality of the prepared samples. On the one hand, Al^{3+} ions form more than one complex with citrate in the solution. Two Al^{3+} ions are bridged by two hydroxyl groups; three of the coordination sites on one of Al^{3+} are occupied by citrate; the last is occupied by water [27]. In this way, the colloidal aluminum forms [28]. On the other hand, some Al^{3+} ions form molecular state of aluminum [29,30].

The gelation of the solution is achieved by the formation of a polymer network, i.e., polyacrylamide, which provides a structural framework to restrain the volume of precursor solution [31]. If the solution only contains acrylamide monomers, which terminate with aminocarbonyl (–$CONH_2$) groups, acrylamide monomers are polymerized in a head-to-tail mode into long polymeric chains [31]. However, when a small amount of bisacrylamide is introduced into the solution, the growing polyacrylamide chains will be cross-linked through the bisacrylamide to grow into a complex web of interconnected loops and branches [32]. By adjusting the pH value to ~7 with aqueous ammonia, hydrolysis and condensation took place in the solution and the complex compounds were encapsulated by a gel network as shown schematically in Fig. 1. This gel network usually has smaller volume and it is structurally stronger than a chain-like gel due to more cross-linkings. Owing to the formation of the three-dimensional (3D) polymer network, the molecular state of aluminum in aqueous solution is trapped within the polymer network, so the mobility of Al^{3+} ions is limited. However, the colloidal state of aluminum in aqueous solution is agglomerated or adhesived on the branches of polymer network and subsequently wraps up the branches to form a wall.

The polymerization reaction is initiated by heating the solution up to 80 °C. The gelation is fast, usually less than 20 min. Finally, the polymer is removed during calcination, the encapsulated aluminum citrate is decomposed during calcinations, resulting in the formation of particles. At the same time, the agglomerated aluminum citrate decomposes and the monolithic structure forms. The pore size and morphology of the samples strongly depend on the chelating agent which is probably because that the different chelating agent will occupy different volume in the gel network after complexing with the cations. Besides, an appropriate amount of glucose is added to the precursor solution to prevent the gel from drastically shrinking during drying [31].

Fig. 2 shows the XRD patterns of Al_2O_3 samples prepared by using citric acid as the chelating agent and calcined at different temperatures. It is clear that the xerogel calcined at 700 °C is cubic γ-Al_2O_3 phase (JCPDS file no. 10-0425). As the calcination temperature is 1000 °C, θ-Al_2O_3 phase is observed. θ-Al_2O_3 is a transition phase, which probably contains major γ-Al_2O_3 phase and minor α-Al_2O_3 phase. The rhombohedral structure of α-Al_2O_3 (JCPDS file no. 35-0121) phase forms completely at 1150 °C and no trace of impurity phases like γ-Al_2O_3 and θ-Al_2O_3 is visible in the XRD pattern.

Fig. 3 shows the XRD patterns of α-Al_2O_3 samples prepared with different chelating agents (EDTA, oxalic acid, tartaric acid and citric acid labeled as S1, S2, S3 and

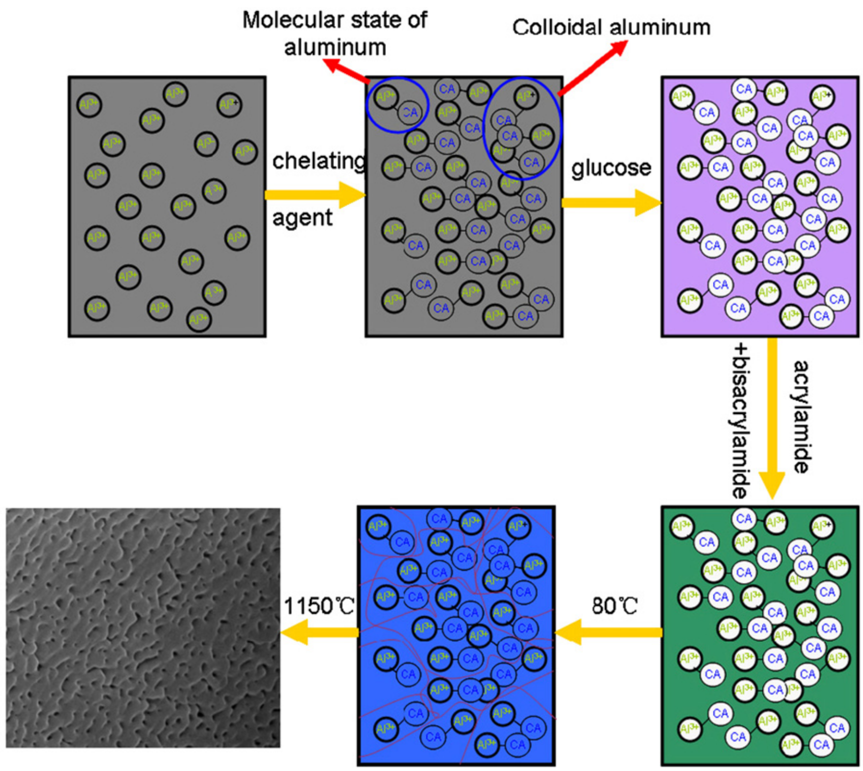

Fig. 1. Scheme for the preparation procedure of monolithic alumina by polyacrylamide gel technique.

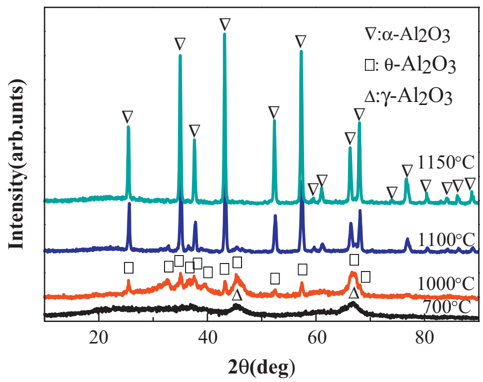

Fig. 2. XRD patterns of Al_2O_3 samples prepared by using citric acid as the chelating agent and sintered at 700, 1000, 1100 and 1150 °C for 1 h.

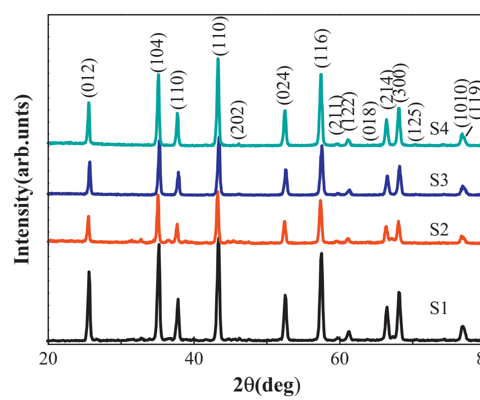

Fig. 3. XRD patterns of α-Al_2O_3 samples prepared by using different chelating agents: EDTA (S1), oxalic acid (S2), tartaric acid (S3) and citric acid (S4).

S4, respectively). The samples are sintered at 1150 °C for 2 h. For the different patterns, all the diffraction peaks can be ascribed to the rhombohedral α-Al_2O_3. It should be noted that all samples are synthesized at the same calcination temperature and time, so the effects of calcination temperature and time on the particle size could be neglected.

The SEM images of the α-Al_2O_3 samples fabricated by different chelating agents are shown in Fig. 4. The α-Al_2O_3 powders exhibit continuously macroporous and monolithic structures, indicating that polyacrylamide can be employed to generate a continuous morphology in the micrometer range. Fig. 5 depicts the corresponding pore size distribution statistically calculated from over 100 pores. The average pore size of S1, S2, S3 and S4 is about 500, 200, 80 and 250 nm, respectively. Interestingly, the pore size of the samples is found to be related to the choice of chelating agent. The prepared α-Al_2O_3 sample has larger pore size when EDTA is used as the chelating agent than others, as shown in Fig. 4. However, the α-Al_2O_3 sample shows isotropic macroporous network when citric acid used as the chelating agent. A typical SEM image of the α-Al_2O_3 network is shown in Fig. 6. This structure makes α-Al_2O_3 a promising candidate as the enhanced mass transportation of chemicals in liquid or biological processes macroporous materials [22].

Fig. 7 shows the photoluminescence spectra of the Al_2O_3 xerogels prepared by using citric acid as chelating agent

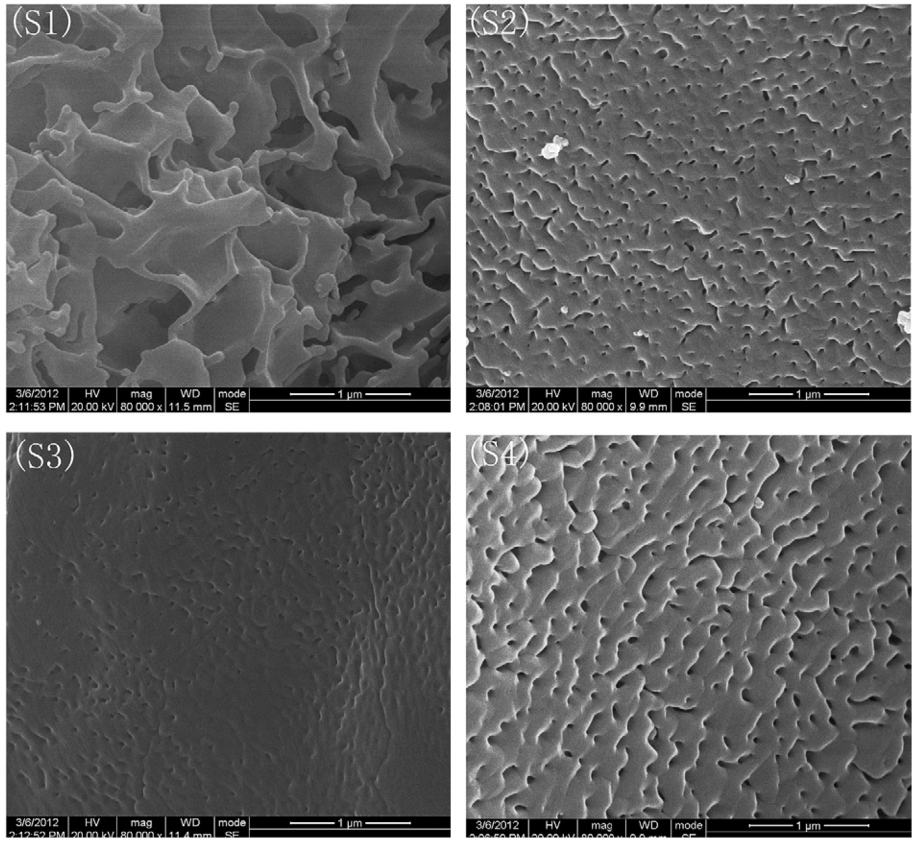

Fig. 4. SEM images of α-Al_2O_3 samples, showing continuous macroporous network.

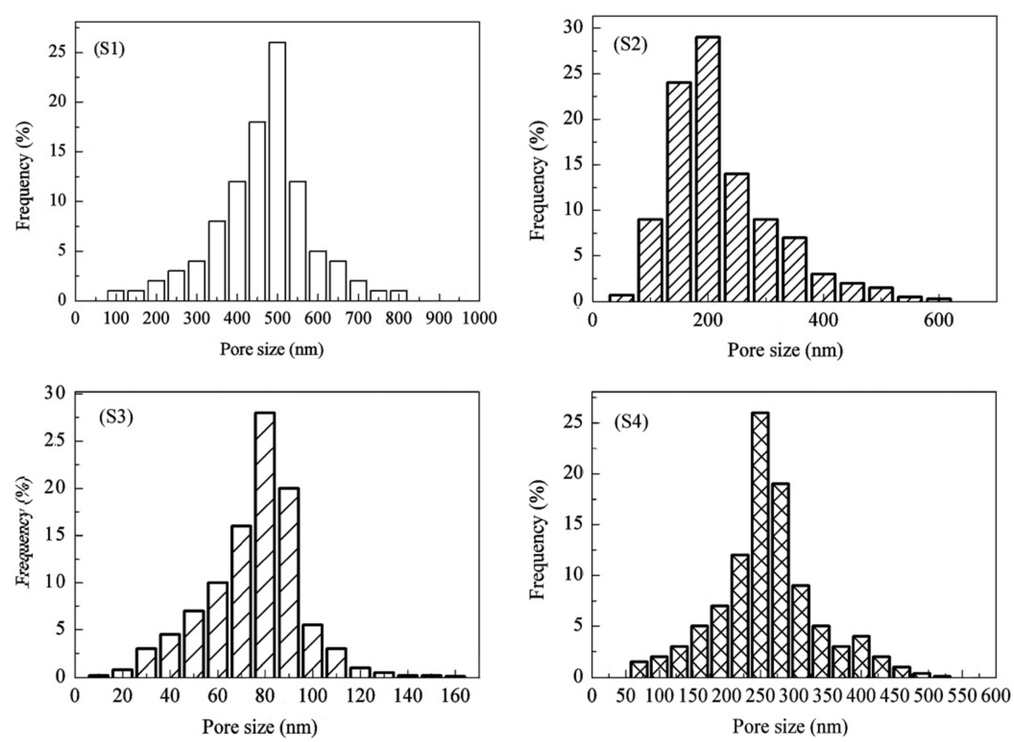

Fig. 5. Pore size distribution of α-Al_2O_3 samples.

and sintered at 700 °C, 1000 °C, 1100 °C and 1150 °C for 2 h, respectively. These spectra were measured with the excitation wavelength of 228 nm. As shown in Fig. 7, for γ-Al_2O_3 sintered at 700 °C, a major emission band around 330 nm is observed, which is probably due to the interaction between the lattice vacancy-type defects (F-, F^+- and

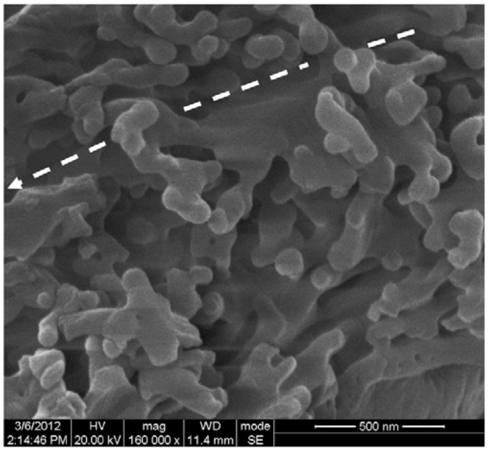

Fig. 6. Typical scanning electron micrograph of the samples prepared by using citric acid as the chelating agent, showing the hierarchical monoliths form in the Al_2O_3 walls. The arrow indicates the direction of the preferential orientation of the macropores.

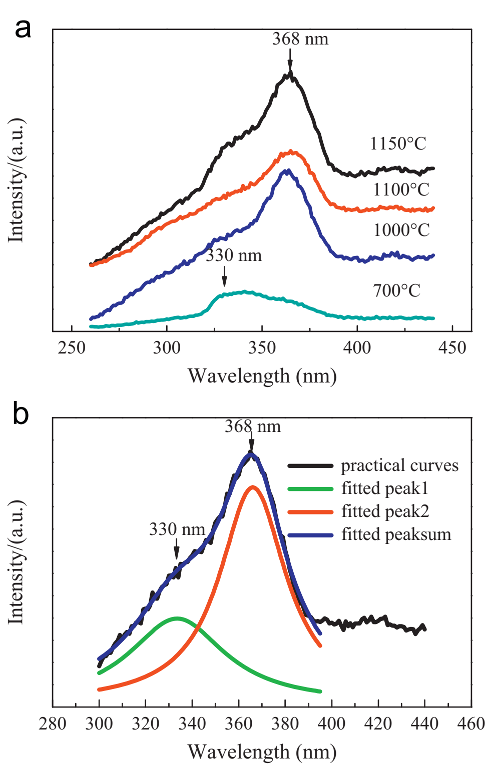

Fig. 7. (a) Photoluminescence spectra (excitation wavelength 228 nm) of Al_2O_3 xerogels prepared by using citric acid as the chelating agent and sintered at different temperatures. (b) Experimental emission spectrum and two Gaussian peaks at 330 nm and 368 nm, respectively.

F_2-type centers) and surface defects of the γ-alumina powder. When the calcination temperature is above 1000 °C, a wide emission band is observed with maximum at 365–368 nm. The PL spectrum of the α-Al_2O_3 is wide and can be resolved by two Gaussian peaks at 330 nm (corresponding to 3.8 eV luminescence is assigned to the $1B \rightarrow 1A$ transation) [33,34] and 368 nm (Fig. 7b). The emission peak at 368 nm could be ascribed to luminescence centers induced by the defects of nonequilibrium phases in the porous materials. It is also possible related to the surface Fs-centers (surface defect level) distributed on the macroporous boundaries [3].

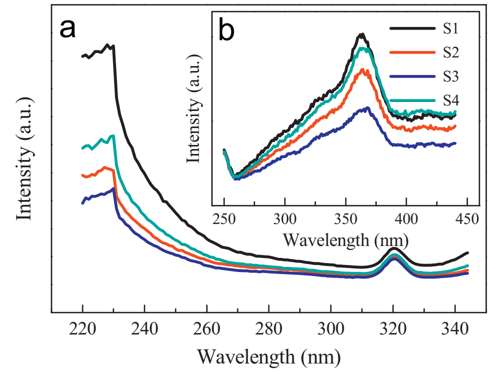

Fig. 8. Excitation (a) and emission (b) spectra of α-Al_2O_3 prepared by using different types of chelating agents and sintered at 1150 °C.

Fig. 8 shows the excitation (a) and emission (b) spectra of α-Al_2O_3 samples prepared by using different chelating agents and sintered at 1150 °C. The excitation peaks at about 228 and 320 nm always occur in the macropores α-Al_2O_3 powder prepared by different chelating agents. The luminescence bands at 330 and 365 nm in the macroporous α-Al_2O_3 powder are present under 228 nm excitation. It is noted that there exists a slight decrease of the luminescence intensity of the peak located at 365 nm when the pore size decreases. Generally, the amount of dangling bonds and unsaturated bonds in the powder surface is heavily dependent on the specific surface area [8]. For the macroporous α-Al_2O_3 powder, the wall size of α-Al_2O_3 increases with the decreasing pore size. The specific surface area of smaller pore is less than that of the larger one so that the number of dangling and unsaturated bonds on the smaller pore surface also decreases. Therefore, the photoluminescence intensity changes with the pore size of α-Al_2O_3 powder.

4. Conclusion

The monolithic α-Al_2O_3 samples with average pore size ranging from 80 to 500 nm have been synthesized by a polyacrylamide gel route. The pore size and morphology of the samples depend on the chelating agent. The luminescence peaks at 330 and 365 nm of the macroporous α-Al_2O_3 powder are observed when the excitation wavelength is 228 nm. The luminescence intensity at 365 nm decreases with the decreasing pore size.

Acknowledgments

This work was supported by the Joint Fund of the National Natural Science Foundation of China and the China Academy of Engineering Physics (Grant no. 11076008) and by the National Natural Science Foundation of China (61178018) and by the Ph.D. Funding Support Program of Education Ministry of China (20110185110007).

References

[1] M. Tahmasebpour, A. Babaluo, S. Shafiei, E. Pipelzadeh, Studies on the synthesis of α-Al_2O_3 nanopowders by the polyacrylamide gel method, Powder Technology 191 (2009) 91–97.
[2] V. Kortov, A. Ermakov, A. Zatsepin, S. Nikiforov, Luminescence properties of nanostructured alumina ceramic, Radiation Measurements 43 (2008) 341–344.
[3] R. Toshima, H. Miyamaru, J. Asahara, T. Murasawa, A. Takahashi, Ion-induced luminescence of alumina with time-resolved spectroscopy, Journal of Nuclear Technology 39 (2002) 15–18.
[4] G.P. Summers, Thermoluminescence in single crystal α-Al_2O_3, Radiation Protection Dosimetry 8 (1984) 69–80.
[5] G.L. Hornyak, C.J. Patrissi, C.R. Martin, Fabrication, characterization, and optical properties of gold nanoparticle/porous alumina composites: the nonscattering Maxwell–Garnett limit, Journal of Physical Chemistry B 101 (1997) 1548–1555.
[6] H. Masuda, K. Fukuda, Ordered metal nanohole arrays made by a two-step replication of honeycomb structures of anodic alumina, Science 268 (1995) 1466–1468.
[7] F. Gu, S.F. Wang, C.F. Song, M.K. Lü, Y.X. Qi, et al., Synthesis and luminescence properties of SnO_2 nanoparticles, Chemical Physics Letters 372 (2003) 451–454.
[8] Z.Q. Yu, C. Li, N. Zhang, Size dependence of the luminescence spectra of nanocrystal alumina, Journal of Luminescence 99 (2002) 29–34.
[9] N. Yao, G. Xiong, Y. Zhang, M. He, W. Yang, Preparation of novel uniform mesoporous alumina catalysts by the sol–gel method, Catalysis Today 68 (2001) 97–109.
[10] D. Han, X. Li, L. Zhang, Y. Wang, Z. Yan, S. Liu, Hierarchically ordered meso/macroporous γ-alumina for enhanced hydrodesulfurization performance, Microporous and Mesoporous Materials 158 (2012) 1–6.
[11] C.L.L. de Faria, T.K.R. De Oliveira, V.L. Dos Santos, C.A. Rosa, J.D. Ardisson, W.A. de Almeida Macêdo, A. Santos, Usage of the sol–gel process on the fabrication of macroporous adsorbent activated-gamma alumina spheres, Microporous and Mesoporous Materials 120 (2009) 228–238.
[12] X. Yuan, S. Xu, J. Lü, X. Yan, L. Hu, Q. Xue, Facile synthesis of ordered mesoporous γ-alumina monoliths via polymerization-based gel-casting, Microporous and Mesoporous Materials 138 (2011) 40–44.
[13] A. Kritikaki, A. Tsetsekou, Fabrication of porous alumina ceramics from powder mixtures with sol–gel derived nanometer alumina: effect of mixing method, Journal of the European Ceramic Society 29 (2009) 1603–1611.
[14] R. Zhao, F. Guo, Y. Hu, H. Zhao, Self-assembly synthesis of organized mesoporous alumina by precipitation method in aqueous solution, Microporous and Mesoporous Materials 93 (2006) 212–216.
[15] T. Isobe, T. Tomita, Y. Kameshima, A. Nakajima, K. Okada, Preparation and properties of porous alumina ceramics with oriented cylindrical pores produced by an extrusion method, Journal of the European Ceramic Society 26 (2006) 957–960.
[16] Y.W. Moon, K.H. Shin, Y.H. Koh, W.Y. Choi, H.E. Kim, Production of highly aligned porous alumina ceramics by extruding frozen alumina/camphene body, Journal of the European Ceramic Society 31 (2011) 1945–1950.
[17] T. Isobe, Y. Kameshima, A. Nakajima, K. Okada, Y. Hotta, Extrusion method using nylon 66 fibers for the preparation of porous alumina ceramics with oriented pores, Journal of the European Ceramic Society 26 (2006) 2213–2217.
[18] Y.W. Moon, K.H. Shin, Y.H. Koh, W.Y. Choi, H.E. Kim, Porous alumina ceramics with highly aligned pores by heat-treating extruded alumina/camphene body at temperature near its solidification point, Journal of the European Ceramic Society 32 (2012) 1029–1034.
[19] C.H. Chen, K. Takita, S. Ishiguro, S. Honda, H. Awaji, Fabrication on porous alumina tube by centrifugal molding, Journal of the European Ceramic Society 25 (2005) 3257–3264.
[20] H.D. Kim, T. Nakayama, B.J. Hong, K. Imaki, T. Yoshimura, T. Suzuki, H. Suematsu, K. Niihara, Fine-structured patterns of porous alumina material fabricated by a replication method, Journal of the European Ceramic Society 30 (2010) 2735–2739.
[21] B. Xu, T. Xiao, Z. Yan, X. Sun, J. Sloan, S.L. González-Cortés, F. Alshahrani, M.L.H. Green, Synthesis of mesoporous alumina with highly thermal stability using glucose template in aqueous system, Microporous and Mesoporous Materials 91 (2006) 293–295.
[22] S.W. Bian, Y.L. Zhang, H.L. Li, Y. Yu, Y.L. Song, W.G. Song, γ-Alumina with hierarchically ordered mesopore/macropore from dual templates, Microporous and Mesoporous Materials 131 (2010) 289–293.
[23] L. Martins, M.A. Alves Rosa, S.H. Pulcinelli, C.V. Santilli, Preparation of hierarchically structured porous aluminas by a dual soft template method, Microporous and Mesoporous Materials 132 (2010) 268–275.
[24] N. Žilková, A. Zukal, J. Čejka, Synthesis of organized mesoporous alumina templated with ionic liquids, Microporous and Mesoporous Materials 95 (2006) 176–179.
[25] Z. Zhang, R.W. Hicks, T.R. Pauly, T.J. Pinnavaia, Mesostructured forms of γ-Al_2O_3, Journal of the American Chemical Society 124 (2002) 1592–1593.
[26] Y. Zhang, H. Liang, C.Y. Zhao, Y. Liu, Macroporous alumina monoliths prepared by filling polymer foams with alumina hydrosols, Journal of Materials Science 44 (2009) 931–938.
[27] N. Mumallah, Chromium (III) Propionate: a crosslinking agent for water-soluble polymers in hard oilfield brines, Society of Petroleum Engineers Reserves and Engineering 3 (1988) 243–250.
[28] C.T. Driscoll, R.D. Letterman, Factors regulating residual aluminum concentrations in treated waters, Environmetrics 6 (1995) 287–305.
[29] S. Meloni, A. Palma, A. Kahn, J. Schwartz, R. Car, Molecular and solid-state (8-hydroxy-quinoline) aluminum interaction with magnesium: a first-principles study, Journal of Applied Physics 98 (2005) 023707.
[30] R.L. Martin, J.D. Kress, I. Campbell, D. Smith, Molecular and solid-state properties of tris-(8-hydroxyquinolate)-aluminum, Physical Review B 61 (2000) 15804.
[31] H. Yang, Z.E. Cao, X. Shen, J.L. Jiang, Z.Q. Wei, J.F. Dai, W.J. Feng, A polymer-network gel route to oxide composite nanoparticles with core/shell structure, Materials Letters 63 (2009) 655–657.
[32] T. Tanaka, Gels, Scientific American 244 (1981) 110–123.
[33] K.H. Lee, J. Crawford, Jr., Luminescence of the F center in sapphire, Physical Review B 19 (1979) 3217.
[34] B.D. Evans, M. Stapelbroek, Optical properties of the F^+ center in crystalline Al_2O_3, Physical Review B 18 (1978) 7089.